Planar waveguide concentrator used with a seasonal tracker

Sébastien Bouchard* and Simon Thibault

Centre d'Optique-Photonique et Laser, 2375, rue de la Terrasse, Quebec City, Quebec G1V 0A6, Canada

*Corresponding author: sebastien.bouchard.6@ulaval.ca

Received 13 June 2012; revised 30 August 2012; accepted 4 September 2012;
posted 5 September 2012 (Doc. ID 170538); published 27 September 2012

Solar concentrators offer good promise for reducing the cost of solar power. Planar waveguides equipped with a microlens slab have already been proposed as an excellent approach to produce medium to high concentration levels. Instead, we suggest the use of a cylindrical microlens array to get useful concentration without tracking during the day. To use only a seasonal tracking system and get the highest possible concentration, cylindrical microlenses are placed in the east–west orientation. Our new design has an acceptance angle in the north–south direction of ±9° and ±54° in the east–west axis. Simulation of our optimized system achieves a 4.6× average concentration level from 8:30 to 16:30 with a maximum of 8.1× and 80% optical efficiency. The low-cost advantage of waveguide-based solar concentrators could support their use in roof-mounted solar panels and eliminate the need for an expensive and heavy active tracker.

OCIS codes: 350.6050, 080.0080, 220.4298.

1. Introduction

The use of concentrated photovoltaics (CPV) was proposed to reduce the cost associated with solar power. With these devices, less expensive cells can be used to produce more power. High-concentration photovoltaic technology requires a precise solar tracker, which makes it inappropriate for roof-mounted panels. Another option is to use low concentration CPV that are fixed but are limited by conservation of etendue [1,2].

The utilization of a planar waveguide as a solar concentrator is quite new and originally came from the design of a planar concentrator [3] combined with backlighting [4]. The idea was developed to make it cost competitive using a roll-to-roll production process [5–7]. In this case, the incident light concentrated by an array of microspherical lenses was coupled into a planar waveguide. The prisms on the back surface are used to couple the rays into the waveguide. Reflecting prisms are habitually used because they offer greater control over the coupling angles than diffuse scattering [8]. The light propagates by total internal reflection in the multimode waveguide to reach the solar cell on the edge. With this concept, the geometrical concentration factor is dependent on the waveguide length [5].

In this paper we propose to change the array of spherical microlenses for an array of cylindrical microlenses. Cylindrical lenses produce a focus line, which makes it possible to eliminate one axis of tracking. This reduces the cost associated with two axes tracking without sacrificing too much collected power [9].

For our analysis we have eliminated the day tracking system. Therefore, the lens needs to have about a ±9° angle of acceptance [half-field of view (HFOV)] in the perpendicular direction to cover the Sun displacement from the zenith and a ±54° in the other axis to cover the sun movement from 8:30 to 16:30.

Using a cylindrical lens is not new and is already used in concentrating systems, whether as a Fresnel lens [10] or as a reflecting system [11]. It has also been mentioned in two patents that a cylindrical lens can be used in combination with a planar waveguide

1559-128X/12/286848-07$15.00/0

[12,13] but without analysis. However, to our knowledge, there exists no previous study of this geometry as a seasonal tracking solar concentrator.

In this work we first establish the limit of attainable concentration for a system that would allow the sun to concentrate from 8:30 to 16:30. This limit is used as an evaluation tool for the planar waveguide concentrator. Second, the effect of using cylindrical lenses instead of spherical lenses is calculated. Finally, the planar waveguide concentrator based on a cylindrical lens slab was modeled in LightTools to evaluate the performance of such a system.

2. Fundamental Limit to Concentration

The conservation of etendue limits the concentration level that can be reached [1,2]. It is related to the field of view θ of the optical system as it appears in Eq. (1):

$$C_{\max} = 1/\sin^2\theta. \tag{1}$$

This limit is attained only for systems designed with nonimaging optics methods. The most well-known example is the compound parabolic concentrator (CPC) [14], whose concentration level can be multiplied by n^2 (index of refraction) if immersed in a dielectric. This approach enables the calculation of the fundamental limit to a concentration that can be expected for a system that would track the sun during this period of the day. So, a rotationally symmetric CPC immersed in a dielectric ($n = 1.7$) would need an acceptance angle of 54° to track the sun from 08:30 to 16:30, which would result in a theoretical concentration factor of 4.4×.

One method to obtain a higher concentration factor for a static CPC was proposed by Winston [11]. It consists of different acceptance angles for each dimension. In this case, the immersed anamorphic CPC would have a 54° HFOV in one axis and 9° HFOV in the other one. With this geometry, the theoretical attainable concentration level would be 13.4× with a 91% optical efficiency for this system for a year-long operation. In our case, this can be considered the ultimate limit to geometric concentration for a day-long static concentrator.

3. From Spherical to Cylindrical Lenses

As previously mentioned, the theoretical limit to concentration is based on the conservation of etendue. A simple spherical imaging lens cannot reach this limit, and its concentration factor is given in Eq. (2):

$$C_{\text{cylind. lens}} = [C_{\text{spher. lens}}]^{1/2} = [1/(2f/\#\tan\theta)^2]^{1/2}. \tag{2}$$

In this case, θ is the HFOV and $f/\#$ is the f number of the lens. By using a cylindrical lens, the concentration factor is the square root of the one for a spherical lens, as shown in Eq. (2) for the same field of view. This is easy to understand because the focus is only in one dimension. If the lens focuses light in a waveguide, the concentration factor is multiplied by the refractive index n of the waveguide.

The focused light is coupled into the waveguide by coupling prism structures. The coupling prisms must be as long as the cylindrical lens to couple the focus line into the waveguide. The total waveguide surface covered by the coupling prisms is much larger than for the spherical microlens array [5]. Consequently, the expected losses will be higher in our approach. The light losses during propagation in the waveguide come from interaction of the light rays with other prism coupling structures. When the rays hit a second prism, the ray propagation angle will change and it can be decoupled from the waveguide. From an analytical model, it is possible to calculate the light lost due to the light propagation within the waveguide using prism coupling structure [5]. The calculation is based on the probability for a ray to be stopped by a coupling prism during the light propagation into the waveguide. We first calculate in Eq. (3) the optical efficiency for rays from an input position P (position within the waveguide) and for the number of surface interactions ($P\tan\phi/2H$). In Eq. (4), the optical efficiency multiplies the reflective coefficient of the coupling prism (R) and the exponential material attenuation (α) along the optical path. Finally, Eq. (5) calculates the total efficiency by including all the cylindrical lenses ($2r$), position (P), and all ray angles (ϕ). The details of this analytical model can be found in [5]:

$$\eta_{\text{decouple}}(P,\phi) = \left(1 - \frac{1}{C_{\text{cylind. lens}}}\right)^{P\tan\phi/2H}, \tag{3}$$

$$\eta_{\text{position}}(P,\phi) = R \times \eta_{\text{decouple}} \times \exp(-\alpha^P/\cos\phi), \tag{4}$$

$$\eta_{\text{total}} = \frac{\sum_P \int_0^{\phi_{\max}} \eta_{\text{position}}(P,\phi)}{(L-r)/2r}. \tag{5}$$

We recall that in these equations, R is the reflection coefficient of the coupling prism, α is the waveguide material attenuation coefficient, H is the waveguide thickness, L is the waveguide length, P is the position inside the waveguide and $2r$ is the pitch of the cylindrical lens. All these parameters are calculated for different waveguide coupling angles Φ and positions P. The coupling angle Φ is integrated over all angles propagating in the waveguide. The lower limit for integration is 0 while the upper limit is $\Phi_{\max}$, as calculated with Eq. (6) using the same parameters as previously defined:

$$\phi_{\max} = 2\left[\theta + \arctan\left(\frac{1}{2nf/\#}\right)\right]. \tag{6}$$

A lateral view of the waveguide with the parameters appearing in the previous equations is

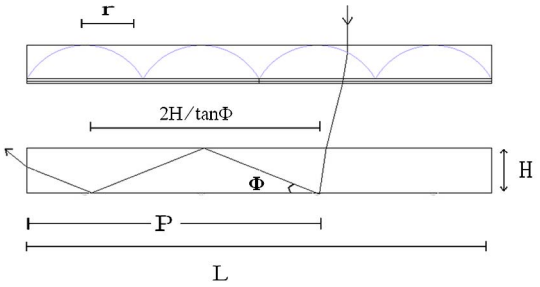

Fig. 1. (Color online) Lateral view of the waveguide with the cylindrical lens slab.

presented in Fig. 1. Compared with the system designed by Karp [5], where the coupling prisms covered less than 0.1% of the total waveguide surface for a 0.26° HFOV, the use of cylindrical lenses would result in prisms covering at least 3% (square root of 0.1%) of the waveguide surface. Consequently, the optical efficiency of the waveguide will be much lower than the Karp system for an equivalent dimension. This is not surprising since we have eliminated a tracking system.

It appears that the most important parameters for optical efficiency are the lens $f/\#$ and the lens field of view. Both are included in the $C_{\text{cylind.lens}}$ parameter of Eq. (3). The influence of the HFOV is presented in Fig. 2, where different angles are tested for an $f/1.2$ lens and a waveguide material with an index of refraction of 1.7, an attenuation coefficient α of 10^{-2} cm^{-1} (based on Schott N-SF15 datasheet), and a reflection coefficient R of 90%.

By looking at Fig. 2A, it is clear that even for a 0.26° HFOV, the losses are quite significant in the waveguide. This can be compared to the 90% optical efficiency obtained by Karp [5] over a 600 mm long waveguide using spherical lenses. Clearly, the efficiency falls rapidly with the increase in the field of view. For this reason, the waveguide needs to be short. In our case, we are mostly interested in the result at 9° HFOV, which is the requirement for our lenses to track the sun from 08:30 to 16:30. According to the model, the optical efficiency of a 10.4 mm long and 1 mm thick waveguide core ($n = 1.7$) is about 64%. The light flux concentration ratio, which is the geometrical concentration (waveguide length/waveguide thickness, 10.4 mm/1 mm) multiplied by the optical efficiency should then be about 6.7×.

The analytical calculation gives a starting point but it also considers that all the guided rays that

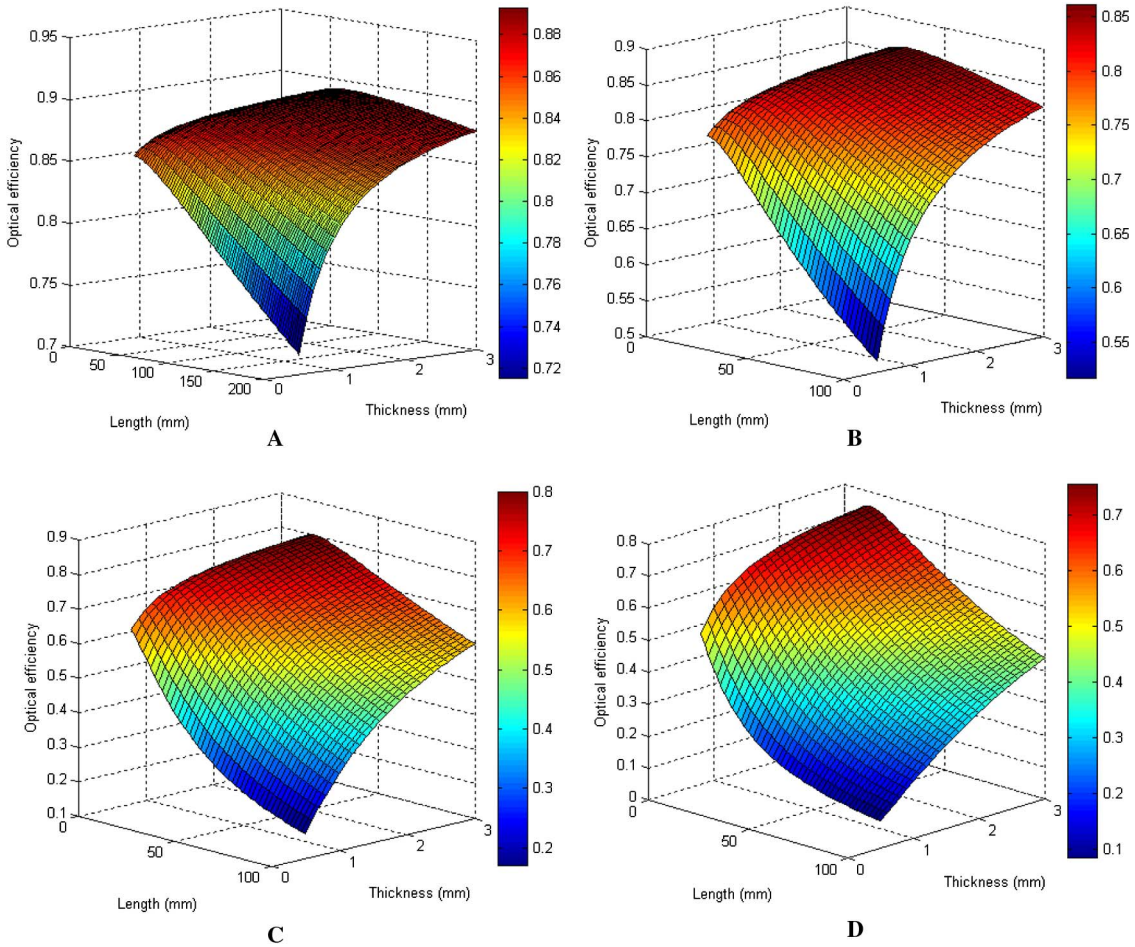

Fig. 2. (Color online) Effect of waveguide length and thickness on optical efficiency of an $f/1.2$ lens for A, 0.26° HFOV; B, 1.26° HFOV; C, 5° HFOV; and D, 9° HFOV.

hit a coupling prism will be lost. We will see in the Section 4 that it is not always the case. This leads to a underestimation of the optical efficiency.

4. Simulation of the System

To illustrate the approach using cylindrical microlenses, we will simulate a particular case. Our goal was to find geometrical parameters for the system which will give an 80% optical efficiency.

The first step was to properly define the coupling structure. As the field of view is large, the coupling prism must be also large enough to maximize the coupling all through the day. From optimization we have defined a particular geometry made from an asymmetric coupling prism. In Fig. 3 we see the optical waveguide definition. The figure also shows that many of the rays are decoupled from the waveguide by striking another prism or because of the spot size (rays miss the coupling prism). These rays are in bold in Fig. 3. However, with the prism geometry used in the design, some rays strike a prism during propagation and still stay in the waveguide. These rays are dotted lines in Fig. 3. The asymmetric coupling prisms are pyramids with two different angles at the base of the waveguide. On one side of the prism the angle is 45°, which sends rays directly toward the output, reducing interactions with the waveguide surface. The other side of the prism has only a 10° angle, which reduces shadowing and losses.

The geometry of the prisms was chosen to maximize light directed toward the output in the middle of the day when the sun is directly perpendicular to the cylindrical lens axis. However, it is possible to choose a different approach. For example, symmetric coupling prism geometry with an angle of 30° on each side would flatten the illumination curve collected over the day. Effectively, in the middle of the day, losses would be higher since surface interactions would be more frequent. At the beginning and at the end of the day, as we will discuss later, the defocus is so important that the coupling angles do not have much effect on the illumination reaching the output. So, over the day, the illumination curve collected would be more flat. The price to pay is a lower concentration level.

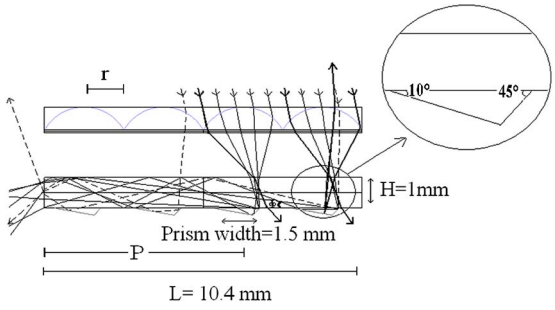

Fig. 3. (Color online) Lateral view of the waveguide with the cylindrical lens slab.

The optical system was modeled and analyzed with LightTools. The complete sun geometry model, including the sun spectrum, makes it the easiest way to evaluate the nontracking possibility and the losses in the planar waveguide. The parameters of the model are presented in Table 1.

The system that was designed is shown in Fig. 4. The cylindrical lens slab is positioned over the waveguide (in air) to have the focus at the bottom of the prism. It is also possible to use defocus as a way to flatten the illumination curve during the day. There is less movement in the spot position but the maximum illumination is lowered. Light concentration should then be lower but more constant during the day.

Figure 5 shows a graph of the optical efficiency of the system (relative illumination reaching the solar cell) during the course of the day. We wanted to have a constant illumination from 8:30 to 16:30 but this is not exactly the case. With the size of the exit aperture of the waveguide that is 30 mm^2 (1 mm × 30 mm), a direct sun level corresponds to a power of 30 mW. This means that the average concentration level is 4.6× with a maximum at 8.1×. The optical efficiency reaches about 78% in the middle of the day when the sun is almost directly over the concentrator. There is a large variation over the course of the day, particularly at the beginning and at the end. At these times, the illumination level is a little over 1 sun.

It needs to be understood that the sun definition of 1000 W/m^2 gives rise to a problem with the optical efficiency over a day-long operation. In fact, it reaches 1000 W/m^2 only around 12:30. There is also a variation during the year between summer and winter. We can compare a panel standing flat on the ground, where the light level can fall to about 500 W/m^2 at the beginning and at the end of the day. This comes from the cosine fourth law, which is illustrated as the relative sun power in Fig. 5. This is the normalized power incident on the aperture of the concentrator during the day. This modifies the real concentration level produced by the system. One method to remove this effect has recently been proposed and is presented in Eq. (7) [15]. It is a ratio of energies at the entrance and at the exit of the system. The numerator is the total energy at the output of the concentrator. The denominator is the total energy incident on the concentrator entrance surface. The idea is to eliminate the variation in the sun intensity from the result, which is essential

Table 1. Parameters of the System Tested in LightTools

Parameter	Value
Waveguide size	10.4 mm × 30 mm
Waveguide core thickness	1 mm
Waveguide refractive index	1.7
Lens $f/\#$	1.2
Coupling prism width	1.5 mm
Lens pitch ($2r$)	2.6 mm

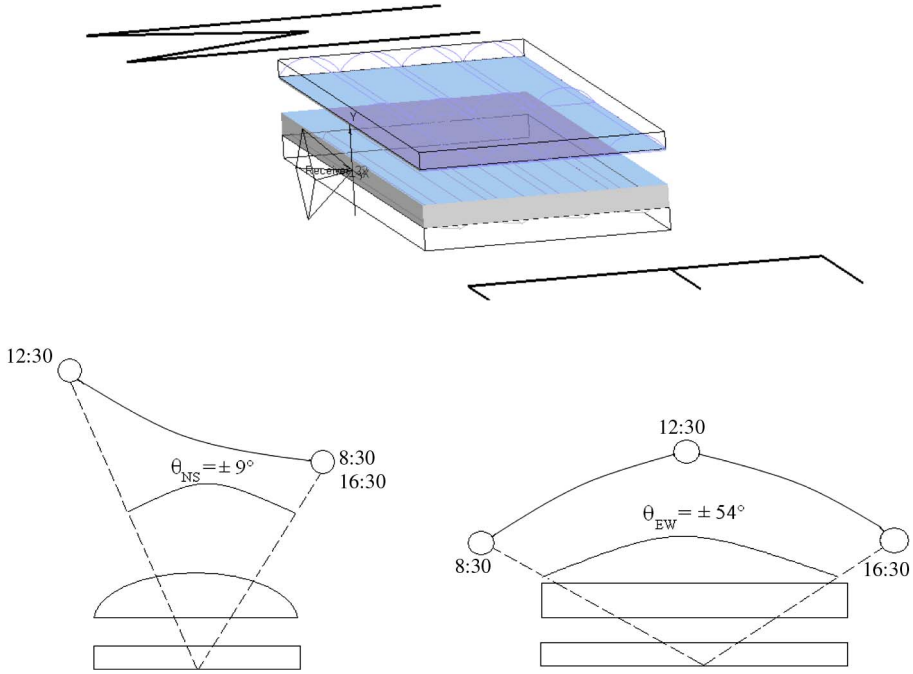

Fig. 4. (Color online) Model of the waveguide concentrator tested in LightTools. The cylindrical lenses are in the east–west (EW) orientation and the waveguide exit side is designated by a pyramid.

to compare the nontracking concentrator over a day-long operation. We chose the limits of integration to fit the period during which the system was designed to concentrate light:

$$P_{\text{ro-eff}} = \frac{\int_{8:30}^{16:30} P_{\text{ro}}[\theta_{\text{NS}}(t), \theta_{\text{EW}}(t)] * P_{\text{Ai}}[\theta_{\text{NS}}(t), \theta_{\text{EW}}(t), t]\mathrm{d}t}{\int_{8:30}^{16:30} P_{\text{Ai}}[\theta_{\text{NS}}(t), \theta_{\text{EW}}(t), t]\mathrm{d}t}, \tag{7}$$

where $P_{\text{ro}}[\theta_{\text{NS}}(t), \theta_{\text{EW}}(t)]$ is the optical efficiency of the concentrator for different sun and panel orientations. $P_{\text{Ai}}[\theta_{\text{NS}}(t), \theta_{\text{EW}}(t), t]$ is the incident power on the concentrator entrance surface for different sun positions. The result is a 50.4% effective optical performance ratio ($P_{\text{ro-eff}}$), which effectively removes the influence of sun variation. This is about 5% better than the average optical efficiency over the day.

According to Fig. 5, it appears that the system reaches a concentration level from 8.1× at 12:30 to 1.1× at 8:30 and 16:30. The maximum concentration level achieved during the day, which is 8.1×, represents about 60% of the limit for a concentrator immersed in a dielectric ($n = 1.7$) as stated in Section 2. This is not a fundamental problem since there is a lot of room to get closer to the limit by using, for example, a second-stage concentrator. The average concentration level is 4.6×, which represents 35% of the two-axis CPC. However, the CPC would have a height of over 23 mm, which is much less compact than the system presented here. The reason for the drop in the illumination level at the beginning and at the end of the day is because the sun becomes too low in the sky. Even if the focus is still in the axis of the coupling prism, the defocus is too important as

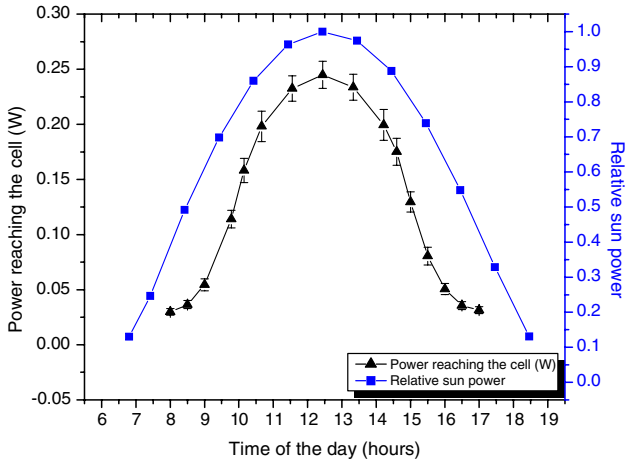

Fig. 5. (Color online) Concentrator performance over the course of the day. The optical efficiency changes depending on the position of the sun in the sky (the error bars are related to the number of rays traced for each point).

illustrated in Fig. 6. One possible method to prevent this would be to give a small curvature to the lens in this axis. This will be looked at in future work.

Now we can compare our simulation result with the analytical model presented in Section 3. Based on Eqs. (3) to (6), the calculated optical efficiency was 64% for our geometry. We have to keep in mind that the model considers sun movement only in the axis perpendicular to the cylindrical lenses. So, the best comparison is at 12:30. In this case, the result is 78% which is better than predicted 64%. We can understand that the analytical model overestimates rays lost because it considers that all the rays that hit the prisms are lost. However, the simulation shows that they are not always ejected and they can still reach the output of the waveguide. There might be some modifications that could be done to the theoretical model to take this effect into account. However, we still consider that the analytical model is a good starting point.

It can be argued that a maximum optical efficiency of 78% (45% on average during the day) is low. Figure 7 presents a simulation of the optical efficiency attained if we changed the waveguide length. There is a need to find a tradeoff between optical efficiency and the concentration factor [16]. A longer waveguide will capture more energy but light will need to travel a longer path in the waveguide, which will reduce optical efficiency. At one point, another microlens will not bring more light at the output. It appears that the overall optical efficiency drops almost linearly as the concentration factor is increasing. For a short waveguide, the theoretical calculation in Fig. 2D underestimates the optical efficiency of the system. For a longer waveguide, this is in good agreement with Fig. 2D, where the optical efficiency is 58% for a 20 mm waveguide. For a longer waveguide, the efficiency drops linearly from 20 mm

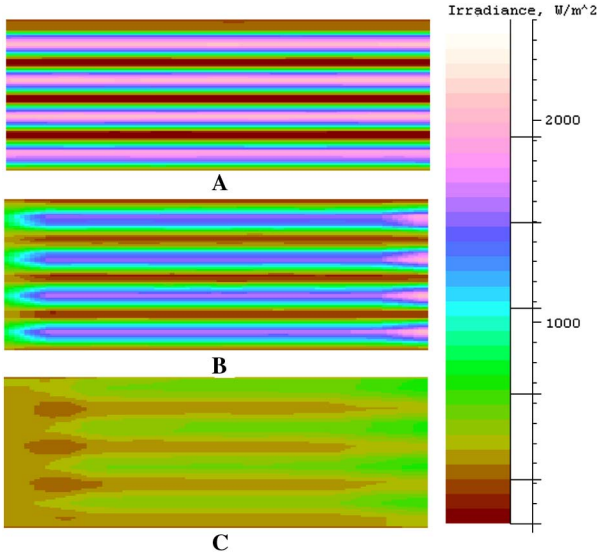

Fig. 6. (Color online) Effect of defocus on the energy distribution on the back of the waveguide (the side with the coupling prisms). A, light is focused on the prisms at 12:30. B, light is spread on a larger surface because of defocus at 14:30. C, focus line is lost at 16:30.

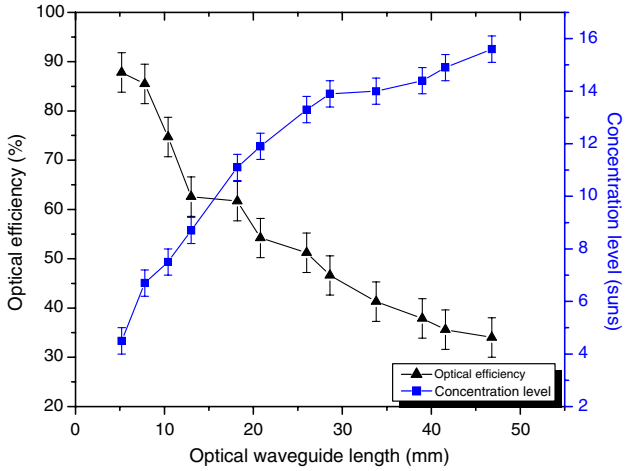

Fig. 7. (Color online) Effect of varying the waveguide length on the optical efficiency of the system at 12:30 (the error bars are related to the number of rays traced for each point).

to about 75 mm, which is similar to Fig. 7. So, the mathematical analysis seems accurate in this range.

However, the 45% average optical efficiency during the day cannot be compared to the prediction from the model. We should consider that at the beginning and at the end of the day, the focus line is above the coupling prisms, as discussed previously and illustrated in Fig. 6. This provides a situation that is not actually taken into account in the theoretical treatment. Consequently, some additional losses come from the impact of low sun elevation at both ends of the day. This effect is quite important and this is why the geometry of the coupling prisms has been chosen to maximize power collected during the middle of the day. This effect will need to be included in the theoretical model.

Another explanation for the difference is the incomplete angular coverage of the exit aperture. This has already been looked at for a waveguide concentrator [6]. To solve this problem, it was proposed to design a second stage concentrator that would extend the angular output. Further concentration could be achieved in the direction perpendicular to the lens axis. Since the light is already coupled in the waveguide, it is possible to design it like a CPC with a 54° acceptance angle. This CPC would have a 1.24× concentration level. So, the total concentration level of our waveguide concentrator based on a cylindrical lens slab should be around 10×. It could be possible to do the same in the system presented here. The major problem is that the movement of the sun parallel to the waveguide makes it harder to design such a secondary concentrator.

5. Conclusion

A planar waveguide concentrator based on a cylindrical lens slab has been simulated and presented in this paper. It can be used as a day-long concentrator where we want to avoid the used of heavy tracking systems. There is still a need for seasonal tracking,

which is easier than precise two-axis tracking usually needed with CPV. It would be an interesting option for roof-mounted solar concentrators.

We show that the cylindrical lens concentration factor is the square root of the factor calculated for standard lenses. The required waveguide is different than the one used in a planar micro-optic system. Particularly, the coupling prism must extend throughout the width of the waveguide to cover the focus line produced by the cylindrical lenses. Consequently, the prism areas and the losses are much larger compared to the planar micro-optic solar concentrator. The model designed in LightTools achieved a maximum concentration level of 8.1× during the day from 8:30 to 16:30 with a nearly 80% optical efficiency. However, the concentration level depends only on the chosen length. It is always possible to trade optical efficiency for a larger concentration level. It corresponds to about 60% of the limit given by the conservation of etendue. This concentration level would come closer to the fundamental limit by designing a secondary stage concentrator. The advantages of this system are the fabrication cost and the possibility to build a thin, lightweight concentrator, given that the concentration level is quite similar to the 7.1× that have been achieved for a commercial CPC used in similar conditions [17]. As suggested by Karp *et al.* [5], the roll processing is possible with low-cost material. This means that the moderate performances are compensated by a very low fabrication cost for mass production that makes a system of this type quite interesting. It could be argued that even with the low-cost fabrication, the optical performance ratio of the system is still too low for economic viability [15]. However, fixed costs for the system, like balance of system and installation, will diminish at the same rate for any design. With concentration, silicon and metal consumption are reduced, which represent 60% of the total materials cost of a flat panel. Additionally, using polymer will also reduce the weight of the system leading also to a cost reduction for the support structure and the installation. So, we decided to evaluate the performance index P of our system [16,18]. This represents the ratio of the cost of a system on the cost of a conventional panel:

$$P = \frac{1}{1+k}\left(\frac{1}{C_g * P_{\text{ro-eff}}}\right) + \frac{k}{1+k}\left(\frac{1}{P_{\text{ro-eff}}}\right), \quad (8)$$

where C_g is the geometrical concentration ratio and $P_{\text{ro-eff}}$ is the previously calculated optical performance ratio during the day. The parameter k is the ratio of cost module (excluding cells) to that of cell production. For a conventional silicon panel $k = 0.43$. We chose to keep this value since our system costs less to produce but requires further installation for seasonal tracking. This gives us a value of $P = 0.73$, which means that the system would be 27% cheaper than conventional panel.

Further work will need to be done to reach the concentration limit. Still, a planar waveguide concentrator with cylindrical lenses shows great potential for roof-mounted systems. We will work on the lens and waveguide shapes to boost optical efficiency, particularly at the beginning and at the end of the day.

This work was supported by the Natural Sciences and Engineering Research Council (NSERC) Industrial Research Chair in Optical Design.

References

1. R. Winston, J. C. Minano, W. T. Welford, and P. Benitez, *Nonimaging Optics* (Academic, 2004).
2. P. Benitez and J. C. Minano, "Concentrator optics for the next-generation photovoltaics," in *Next Generation Photovoltaics*, A. Martí and A. Luque, eds. (Institute of Physics, 2004), Chap. 13, pp. 285–322.
3. M. C. Chien, Y. L. Tung, and C. H. Tien, "Ultracompact backlight-reversed concentration optics," Appl. Opt. **48**, 4142–4148 (2009).
4. R. Winston and J. M. Gordon, "Planar concentrators near the étendue limit," Opt. Lett. **30**, 2617–2619 (2005).
5. J. H. Karp, E. J. Tremblay, and J. E. Ford, "Planar micro-optic solar concentrator," Opt. Express **18**, 1122–1133 (2010).
6. J. H. Karp, E. J. Tremblay, J. M. Hallas, and J. E. Ford, "Orthogonal and secondary concentration in planar micro-optic solar collectors," Opt. Express **19**, A673–A685 (2011).
7. W. C. Shieh and G. D. Su, "Compact solar concentrator designed by minilens and slab waveguide," Proc. SPIE **8108**, 81080H (2011).
8. J. G. Chang and Y. B. Fang, "Dot-pattern design of a light guide in an edge-lit backlight using a regional partition approach," Opt. Eng. **46**, 1–9 (2007).
9. S. Abdallah, "The effect of using sun tracking systems on the voltage-current characteristics and power generation of flat plate photovoltaics," Energy Convers. Manage. **45**, 1671–1679 (2004).
10. C. J. Sletten, F. S. Holt, and S. B. Herskovitz, "Wide-angle lenses and image collapsing subreflectors for nontracking solar collectors," Appl. Opt. **19**, 1439–1453 (1980).
11. R. Winston and W. Zhang, "Pushing concentration of stationary solar concentrators to the limit," Opt. Express **18**, A64–A72 (2010).
12. M. A. Raymond, H. G. Lange, and S. Weiss, "Lens system with directional ray splitter for concentrating solar energy," U.S. patent application 20110079267A1 (1 Oct. 2010).
13. J. E. Ford, J. H. Karp, E. J. Tremblay, and J. M. Hallas, "System and method for solar energy capture and related method of manufacturing," World Intellectual Property Office application WO 2010/033859 A2(18 Sept. 2010).
14. R. Winston, "Light Collection within the framework of geometrical optics," J. Opt. Soc. Am. **60**, 245–247 (1970).
15. G. Grasso, A. Righetti, M. C. Ulbadi, F. Morichetti, and S. M. Pietralunga, "Competitiveness of stationary planar low concentration photovoltaic modules using silicon cells: A focus on concentrating optics," Solar Energy **86**, 1725–1732 (2012).
16. J. M. Kim and P. S. Dutta, "Optical effiency-concentration ratio trade-off for a flat panel photovoltaic system with diffuser type concentrator," Sol. Energy Mater. Sol. Cells **103**, 35–40 (2012).
17. K. A. Shell, S. A. Brown, M. A. Schuetz, B. J. Davis, and R. H. French, "Performance of a low-cost, low-concentration photovoltaic module," AIP Conf. Proc. **1407**, 146–149 (2011).
18. K. Yoshioka, K. Koizumi, and T. Saitoh, "Simulation and fabrication of flat-plate concentrator modules," Sol. Energy Mater. Sol. Cells **75**, 373–380 (2003).